Clim Dyn (2012) 39:1841–1857
DOI 10.1007/s00382-012-1460-7

# Seasonal climate information preserved in West Antarctic ice core water isotopes: relationships to temperature, large-scale circulation, and sea ice

**Marcel Küttel · Eric J. Steig · Qinghua Ding · Andrew J. Monaghan · David S. Battisti**

Received: 19 June 2011 / Accepted: 14 July 2012 / Published online: 31 July 2012


**Abstract** As part of the United States' contribution to the International Trans-Antarctic Scientific Expedition (ITASE), a network of precisely dated and highly resolved ice cores was retrieved from West Antarctica. The ITASE dataset provides a unique record of spatial and temporal variations of stable water isotopes ($\delta^{18}$O and $\delta$D) across West Antarctica. We demonstrate that, after accounting for water vapor diffusion, seasonal information can be successfully extracted from the ITASE cores. We use meteorological reanalysis, weather station, and sea ice data to assess the role of temperature, sea ice, and the state of the large-scale atmospheric circulation in controlling seasonal average water isotope variations in West Antarctica. The strongest relationships for all variables are found in the cores on and west of the West Antarctic Ice Sheet Divide and during austral fall. During this season positive isotope anomalies in the westernmost ITASE cores are strongly related to a positive pressure anomaly over West Antarctica, low sea ice concentrations in the Ross and Amundsen Seas, and above normal temperatures. Analyses suggest that this seasonally distinct climate signal is due to the pronounced meridional oriented circulation and its linkage to enhanced sea ice variations in the adjacent Southern Ocean during fall, both of which also influence local to regional temperatures.

**Keywords** Antarctica · Ice cores · Water isotopes · Diffusion · Sea ice · Temperature · Atmospheric circulation

**Electronic supplementary material** The online version of this article (doi:10.1007/s00382-012-1460-7) contains supplementary material, which is available to authorized users.

M. Küttel · E. J. Steig (✉) · Q. Ding
Department of Earth and Space Sciences and Quaternary Research Center, University of Washington, Seattle, WA 98195, USA
e-mail: steig@uw.edu

M. Küttel
e-mail: mkuettel@uw.edu

A. J. Monaghan
National Center for Atmospheric Research, Boulder, CO 80307-3000, USA

D. S. Battisti
Department of Atmospheric Sciences, University of Washington, Seattle, WA 98195, USA

## 1 Introduction

The instrumental climate record from Antarctica is among the shortest, with most series only starting in 1957. Although there have been considerable efforts to develop spatially complete data sets (Chapman and Walsh 2007; Monaghan et al. 2008; Steig et al. 2009), knowledge of Antarctic climate variability prior to the mid-20th century is mainly restricted to proxy information extracted from ice cores.

Since the pioneering studies by Epstein et al. (1963) and Dansgaard (1964), oxygen and deuterium isotope ratios ($\delta^{18}$O and $\delta$D, hereafter referred to collectively as $\delta$) preserved in snow and ice have commonly been used to assess past variations in Antarctic climate. While $\delta$ is often considered a paleothermometer, there are a number of factors influencing the isotopic composition of accumulated snow and ice such as changes in source region, transportation path, timing of precipitation, and post-depositional alterations, all significantly modifying the relationship between $\delta$ and temperature (e.g. Noone and Simmonds 2002a; Masson-Delmotte et al. 2008). Accordingly, the correlation between local temperature and $\delta$ is either low or the regression slope varies significantly over time at some

locations (e.g. Epstein et al. 1963; Schneider and Noone 2007; Sime et al. 2009). Other studies suggest that significant correlations between $\delta$ and temperature in Antarctica mostly arise from the covariance of temperature and precipitation amounts (Noone and Simmonds 2002a), or the covariance of temperature and sea ice concentrations (Bromwich and Weaver 1983). In order to correctly interpret past $\delta$-variations a comprehensive understanding of the various influences affecting changes in isotopic compositions is therefore needed.

There exist several studies relating isotopic variations across Antarctica to the state of the large-scale atmospheric circulation, indicating that this relationship is complex, possibly varies over time, and is often modified by the El Niño Southern Oscillation (ENSO). Focusing on the very strong positive $\delta$-anomaly found in West Antarctic ice cores in 1941, Schneider and Steig (2008) demonstrate that this event can be related to a persistent positive pressure anomaly offshore, which they suggest was induced by a strong El Niño event with particularly pronounced warming in the central tropical Pacific. Some studies (Schneider and Noone 2007; Gregory and Noone 2008; Divine et al. 2009), using $\delta$-records from various parts of Antarctica, find a signature of the quasi zonally-symmetric Southern Annular Mode (SAM) as well as of ENSO. They note, however, that the relationship to ENSO is intermittent and strongly dependent on the state of the SAM. Other studies show that neither SAM nor ENSO are necessarily the most useful measure of the relevant dynamics controlling isotope variations in Antarctica. For example, Schneider et al. (2004, 2012), Steig et al. (2009), and Ding et al. (2011) find that temperature variations and trends in West Antarctica are related to the zonally asymmetric wavenumber three and Pacific South American (PSA) patterns (Mo and Ghil 1987).

Changes in sea ice concentrations are also commonly cited as a major contributor to Antarctic $\delta$-variations (e.g. Bromwich and Weaver 1983; Grootes and Stuiver 1986; Thomas and Bracegirdle 2009). The modeling study by Noone and Simmonds (2004) provides a general framework for understanding the influence of sea ice on stable water isotopes and shows that a reduction of sea ice concentration directly changes $\delta$ through the injection of relatively enriched water vapor and also indirectly by reducing, through an increased sensible heat flux, the stratification of the air mass aloft thus allowing the air masses to penetrate deeper into the continent. Noone and Simmonds (2004) accordingly argue that particularly the coastal areas of Antarctica are sensitive to sea ice changes. In contrast, the more interior parts of the continent are less sensitive to sea ice changes since they receive moisture mostly through large-scale transportation, which has few interactions with the ocean surface near Antarctica (Noone and Simmonds 2002b, 2004). In practice, separating the influence of sea ice and atmospheric circulation is difficult because they are highly correlated (Cavalieri and Parkinson 1981; White and Peterson 1996; Stammerjohn et al. 2008; Turner et al. 2009; Schneider et al. 2012).

With various factors acting upon the composition of stable water isotopes in precipitation, a network of well distributed and precisely dated ice core profiles is needed to fully represent isotope variation and its relationship to climate. This is particularly true for West Antarctica where topographic boundaries formed by the main ice drainage divides are expected to further influence the precipitation distribution (Kaspari et al. 2004; Steig et al. 2005; Nicolas and Bromwich 2011). Here, a network of eight precisely dated and spatially well distributed $\delta$-records from West Antarctica is related, on a seasonal time scale, to temperature, large-scale atmospheric circulation, and sea ice concentrations. These records represent a unique opportunity both to assess the climate signal preserved in West Antarctic ice cores with high temporal resolution and to determine how and why the climatic signal varies spatially.

This paper is structured as follows: Sect. 2 introduces the data and methods used, focusing on the technique applied to account for the effect of water vapor diffusion. Section 3 presents the results. We find that the year 1980 manifests a prime example where the joint influence of sea ice and atmospheric circulation on stable water isotopes is unambiguously captured in the ice core records. We also show that the cores located in the western part of West Antarctica contain the strongest climate signal, particularly in the austral fall season. Section 4 discusses the results, puts them into context with earlier studies, and presents implications for paleoclimatic reconstructions from West Antarctic ice core water isotopes.

## 2 Data and methods

We use water isotope data collected under the United States' contribution to the International Trans-Antarctic Scientific Expedition (ITASE; Mayewski et al. 2005), atmospheric circulation data from ERA40 (Uppala et al. 2005), sea ice data from HADISST (Rayner et al. 2003), and instrumental temperature from Byrd Station. Since the majority of the ice core records considered here end in 1999 (Sect. 2.1) and the climate data at high southern latitudes are reliable only from 1979 onwards (Sect. 2.2), we limit our analysis primarily to the 1979–1999 period.

### 2.1 ITASE cores

We use isotopic measurements ($\delta^{18}$O and $\delta$D) from shallow, highly resolved ice cores drilled across West Antarctica. The isotopic concentrations were obtained at the

University of Washington by mass spectrometry, using $CO_2$-equilibration and reduction on chromium; all data are available through the United States National Snow and Ice Data Center (Steig 2009). Description of the analytical methods are given in Steig et al. (2005), Schneider et al. (2005) and references therein. Eight cores are selected on the basis of their length (at least extending back to 1900) and degree of isotope diffusion; these are US ITASE cores 2000–1, 2000–4, 2000–5, 2001–2, 2001–3, 2001–5, 2002–2, and 2002–4. The top $\sim$1–2 m of the isotope profiles are from uncompacted snow, which is more difficult to sample. We therefore neglect this top part, thereby losing 1–5 years of the most recent period. This shortens most records to 1999, and core 2002–4 to 1997. We extend core 2002–4 to 1999 using the adjacent snow pit data. We find excellent agreement between ice core and snow pit $\delta^{18}$O and $\delta$D in the overlapping period. Both $\delta^{18}$O and $\delta$D are available for most cores; we select either of them depending on which of the two time series is more complete. Because they are effectively identical (scaled by a factor of 8) we do not generally distinguish $\delta^{18}$O and $\delta$D in the text, using '$\delta$' to refer to either one. The deuterium excess parameter ($d = \delta D - 8{*}\delta^{18}O$) is of interest but is not considered here because the differential diffusivity of $\delta^{18}$O and $\delta$D (Johnsen et al. 2000) makes it impossible to meaningfully relate sub-annual $d$ variations in these cores to the original composition at the surface. Similarly, we do not consider accumulation variations since sub-annual information, which is of primary interest here, cannot be obtained from the accumulation time series. While Kaspari et al. (2004) report a climatic signal in the annual accumulation time series of the ITASE cores, we do not find any clear relationship between accumulation and $\delta$ on annual time scale. This point towards different key drivers behind variations in accumulation and $\delta$ and should be further explored in future research.

Dating of the ITASE cores is primarily based on identifying the austral summer peaks in non-sea-salt sulfate ($nssSO_4^{2-}$), nominally assigning it to 1 January (see Dixon et al. 2004 and Steig et al. 2005 for details). We calculated monthly averages by linearly interpolating between the summer peaks, assuming a constant accumulation rate throughout the year. While this assumption may not be strictly valid, Bromwich et al. (2004) report seasonal variations in snowfall amounts across West Antarctica to be smaller than 25 %. Furthermore, Steig et al. (2005) use the in-phase occurrence of $nssSO_4^{2-}$ with peaks in summer nitrate and stable isotopes along with other indicators to demonstrate that the precision of the assignment of months is $\pm$1 month. Schneider et al. (2005) show that the seasonal isotopic cycle in the ITASE cores is highly significantly ($r > 0.9$) correlated with the local seasonal temperature cycle, both showing a broad minimum in austral winter.

Although there are several other highly resolved $\delta$ time series available from West Antarctica, we restrict our analysis to the ITASE cores, since this dataset has the crucial advantage that the dating was conducted by the same investigators, using the same methodology for all cores and also putting much emphasis on accurate cross-dating of the cores (Dixon et al. 2004). We also do not include the WDC05A core of the West Antarctic Ice Sheet (WAIS) Divide project (White and Steig unpublished data), but we note that the results presented here are maintained when including this particular core, and are therefore relevant to the interpretation of the deep ice core which was recently drilled at WAIS Divide. Figure 1 illustrates that the ITASE cores are a good spatial representation of West Antarctica with cores located on (core 2000–1), east (2001–3, 2001–5), west (2000–4, 2000–5), as well as south (2001–2, 2002–2, 2002–4) of WAIS Divide. This is important considering that the pronounced topography (Fig. 1) along with the various circulation systems affecting West Antarctica (Sect. 1) are expected to significantly alter the distribution of precipitation and its isotopic composition across this region. Characteristics of the cores are given in Table 1.

### 2.1.1 *Forward diffusion of the ITASE δ-profiles*

While the accumulation rates in West Antarctica (Table 1) are generally high enough that isotopic diffusion may be

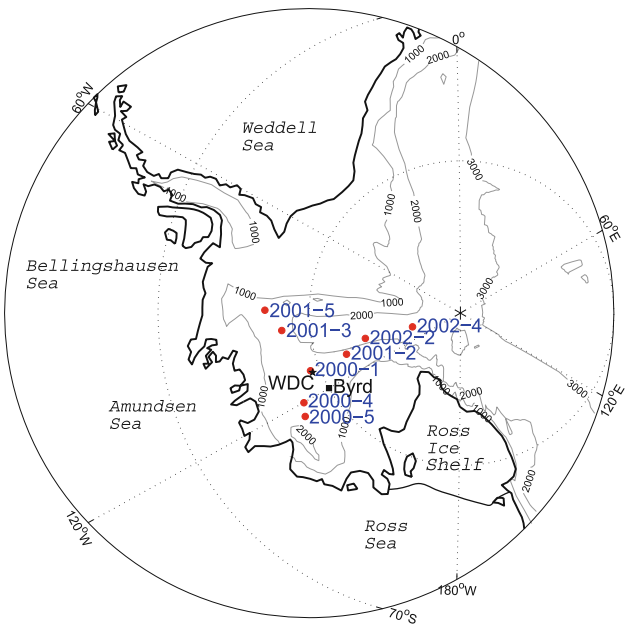


**Fig. 1** Locations of the ITASE cores (*red dots*), Byrd Station (*black rectangle*), and the West Antarctic Ice Sheet Divide core (WDC; *black star*). *Contour lines* indicate the topography of West Antarctica [meters above sea level] as derived from the ETOPO2 dataset (available at the Research Data Archive from the National Center for Atmospheric Research)

**Table 1** Overview of the ITASE records considered in this study

| Core name | 2000–1 | 2000–4 | 2000–5 | 2001–2 | 2001–3 | 2001–5 | 2002–2 | 2002–4 |
|---|---|---|---|---|---|---|---|---|
| Longitude | 111.24°W | 120.08°W | 124°W | 110.01°W | 95.65°W | 89.14°W | 104.99°W | 107.99°W |
| Latitude | 79.38°S | 78.08°S | 77.68°S | 82°S | 78.12°S | 77.06°S | 83.5°S | 86.5°S |
| Elevation (m) | 1791 | 1697 | 1828 | 1746 | 1620 | 1239 | 1957 | 2586 |
| Accumulation (cm $a^{-1}$ w.e.) | 20.12 | 17.37 | 12.89 | 39.06 | 29.84 | 35.58 | 33.45 | 10.1 |
| Full length of record | 1673–2001 | 1789–1999 | 1718–2001 | 1891–2002 | 1858–2000 | 1779–2000 | 1894–2001 | 1592–1999 |
| Isotope analyzed | $\delta$D | $\delta^{18}$O | $\delta$D | $\delta^{18}$O | $\delta$D | $\delta^{18}$O | $\delta^{18}$O | $\delta$D |
| Mean annual temperature (°C) | −27.87 | −27.39 | −27.83 | −26.82 | −25.53 | −26.57 | −29.31 | −40.71 |

The accumulation is calculated over the 1961–1990 period, the mean annual temperature over 1979–1999 using the ERA40 2-m temperature (Uppala et al. 2005) at the grid box co-located with the ITASE cores

neglected at annual time scales (see e.g. Cuffey and Steig 1998), its impact must be accounted for in interpretations of seasonal data. Damped frequencies in the isotopic profile can in principle be restored using deconvolution as introduced by Johnsen (1977). However, Cuffey and Steig (1998) found that while deconvolution was useful as an aid in dating ice cores using seasonal isotope variations, it provides little additional information on seasonal anomalies. Furthermore, small dating and measurement errors in the record are amplified by back-diffusion, potentially leading to spurious correlations. Hence, we choose here to forward-diffuse the isotopic profiles; that is, we smooth the records with appropriate filters such that the amplitude of the seasonal $\delta$ anomalies is equally damped throughout all ice core profiles. We note that this procedure will tend to increase the autocorrelation in the data, but that this can be accounted for by appropriately reducing the degrees of freedom in the calculation of significance levels of correlations (Bretherton et al. 1999). Details of the forward-diffusion approach are given next. Vinther et al. (2010) applied a similar approach to ice core $\delta$ records from Greenland.

First, in order to determine how far back in time the annual cycle in the water isotopes is detectable at a statistically significant level ($p \leq 0.05$), we subject all eight ITASE $\delta$-profiles to a wavelet spectral analysis, following the methodology outlined in Torrence and Compo (1998). As expected and as stated in Steig et al. (2005), the annual cycle is detectable throughout the entire record (up to 220 years) in the high accumulation cores located east of WAIS Divide (cores 2001–3 and 2001–5), while it is rapidly lost in the lower accumulation cores west of the divide (minimum extent: 50 years in core 2000–5). This determines the maximum year to which we expect sub-annual information to be preserved.

Next, we estimate the degree of diffusive smoothing by empirically determining the diffusion length $\sigma$ at each month $t$ as (Johnsen et al. 2000)

$$\sigma_{(t)} = \sqrt{\frac{-2\lambda_{(t)}^2 \ln\left(\frac{A_{(t)}}{A_0}\right)}{4\pi^2}} \quad (1)$$

where, $t$: time at a given depth in the core, with $t = 0$ at the surface, $\lambda$: wavelength of the harmonic cycle (12 months), $A_{(t)}/A_0$: ratio of the amplitude of the annual cycle at time $t$ to the initial amplitude $A_0$ (relative amplitude).

Here, the initial amplitude of the annual cycle is defined as the maximum amplitude of the record. The maximum amplitude is not always found in the very top of the record, but always within the most recent few years. The assumption is necessarily made that the initial amplitude of the seasonal cycle is constant. In order to avoid spurious noisy estimates of diffusion length due to variations in the seasonal timing of snowfall, sampling error etc. and to rather obtain the long-term changes in annual cycle amplitude, we smooth the time series of relative amplitude with a 31-year running mean; for the uppermost layers, we use a progressively shorter averaging window, with the uppermost layer being a 15-year average. We use a 31-year smoothing since this is a standard time window for 'climatological' estimates. We emphasize, however, that our results are not sensitive to the choice of the window length. Using a shorter window length (e.g. 7 or 15 years) does not change our results (Suppl. Figs. 1 and 2). The diffusion length $\sigma$ represents the characteristic distance over which the isotopic signal has been smoothed due to the molecular diffusion of water vapor, and is related to the depth-dependent diffusivity of water vapor in firn, $D$, by

$$\sigma(t) = \frac{dt}{dz}\left(4t\frac{1}{z(t)}\int_0^{z(t)} D dz\right)^{0.5} \quad (2)$$

where $z$ is depth. Note that as defined here, $\sigma$ has units of time, rather than depth, because it is estimated from the time-profiles, rather than depth-profiles, of the isotopic variations. Also, the diffusivity $D$ here implicitly includes

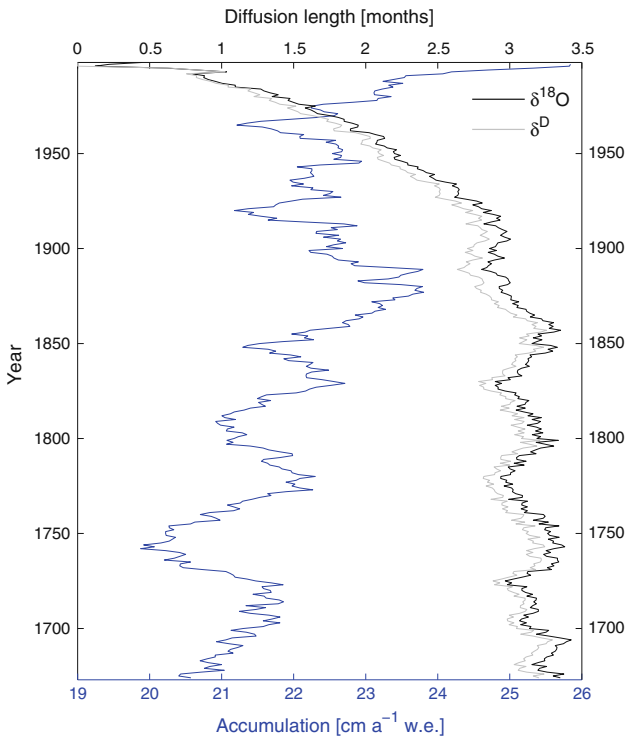


**Fig. 2** Annual diffusion length $\sigma$ [months] calculated for $\delta^{18}O$ (*black line*) and $\delta D$ (*gray line*) of the ITASE 2000–1 core, along with the annual accumulation rate (cm $a^{-1}$ water equivalent; smoothed with a 31-year running mean; *blue line*) at this site

the influence of vertical strain (see Johnsen 1977; Cuffey and Steig 1998; Johnsen et al. 2000 for extensive discussions of isotope diffusion in firn).

Figure 2 presents the calculated diffusion length for the ITASE 2000–1 core, along with the accumulation time series, showing that the diffusion length increases rapidly for the upper ~80–100 years (corresponding to 30–35 m depth in this particular core), but shows a strong relationship to accumulation rates thereafter. This relationship is expected since a higher annual accumulation means that the diffusion affects a shorter time interval in the firn (see also Supp. Fig. 1). Notably and as expected from the different fractionation factors (Johnsen et al. 2000), the diffusion length derived for $\delta D$ is smaller than for $\delta^{18}O$; that is the former is slightly less affected by diffusion than the latter. We also note that the calculated ratio in diffusion length between $\delta D$ and $\delta^{18}O$ is very similar (averaging ~ 0.95) to what is expected from theory (Johnsen et al. 2000).

Next, we apply additional diffusive smoothing to each record, such that all data in all records have been subject to the same amount of smoothing. That is, the largest diffusion lengths of *all* eight ITASE records is determined and the original time series $\delta_{measured}$ are additionally smoothed by convolving them with the filter $f_{add}$

$$\delta_{\text{diffused}} = f_{\text{add}} * \delta_{\text{measured}} \quad (3)$$

where * denotes convolution. The filter, $f_{add}$ is the normalized Gaussian, following Johnsen et al. (2000):

$$f_{add}(\tau) = \frac{1}{\sigma_{add}\sqrt{2\pi}} \exp(-0.5\tau^2/\sigma_{add}^2) \quad (4)$$

where $\sigma_{add}^2(t) = \sigma^2(t_{\max}) - \sigma^2(t)$.

Note that $f_{\text{add}}$ is a function of time (i.e., of depth in the core) and thus the convolution is calculated separately for each month $t$. See the electronic supplementary material for more details and derivation of these relationships.

Importantly, the maximum diffusion length $\sigma(t_{\max})$ found in all cores back to 1979 is ~1.5 months, based on the 31-year smoothed estimates, and ~2.5 months based on shorter window lengths. That is, the isotope signal on time scales longer than a few months will not be appreciably influenced by the diffusion of water vapor, though the $\delta$-values at the edges of the seasons may be slightly mixed due to diffusion. We therefore use 3-month average isotopic values in the cores, after correctly forward diffusing the time series. Figure 3 presents the eight monthly-resolved ITASE cores before and after diffusing them to 1979, illustrating that the changes are small and generally restricted to the most recent few years. Note that we could include the additional core US ITASE 1999-1 in our study if we were to accept larger values for $\sigma(t_{\max})$. We have chosen not to include this record due to the low elevation and accumulation at this site (see also Steig et al. 2005), but note that including this core does not qualitatively change our results. Similarly, in the southernmost core (2002–4), the generally low accumulation rates (see Table 1) mean that isotopic information is expected to be mixed across seasonal boundaries during years with particularly low accumulation. Consequently, this core is not used for in-depth analysis of the seasonal climate information preserved in the ITASE cores, but is included in the more general analysis on annual time scale or for single years in order to have a spatially more complete picture. Finally, some of the winter minima in the low-accumulation core 2000–5 might be obscured by diffusion (Fig. 3). We nevertheless opt to include this particular core in the sub-annual analysis note, however, that excluding this core does not significantly alter our results (see Sect. 3).

## 2.2 Reanalysis and observational data

We investigate the relationships of seasonal isotopic variability in the ITASE cores to the atmospheric circulation over Antarctica, sea ice variations offshore of West Antarctica, and local and regional temperatures. For circulation, we use the ERA40 500 hPa geopotential heights (hereafter Z500) south of 30°S (Uppala et al. 2005) and for

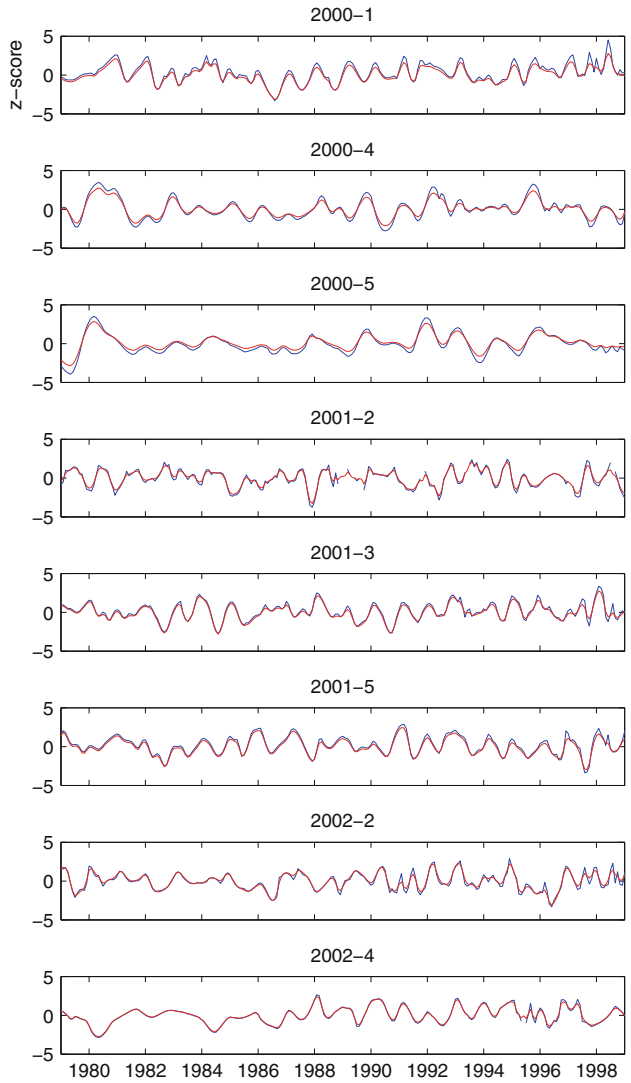


**Fig. 3** Original (*blue*) and forward-diffused (*red*) monthly resolved and standardized $\delta^{18}O/\delta D$ values 1979–1999 of the eight ITASE cores used in this study. Table 1 lists the isotope used for each core

sea ice the fractional sea ice coverage off West Antarctica (180°–70°W) from the HadISST data set (Rayner et al. 2003). Choosing pressure levels other than 500 hPa yields similar results. Selecting the regional area of the sea ice field leads to slightly better organized spatial patterns than using the entire hemisphere with the results presented here not being dependent on this selection. To characterize the dominant circulation and sea ice modes, empirical orthogonal function (EOF) analysis is performed on the covariance matrix of the latitude-weighted climate fields. This is done separately for each season: austral summer (DJF), fall (MAM), winter (JJA), and spring (SON). The linear trend is removed prior to EOF analysis; this has a significant effect only on the patterns derived for austral spring and summer sea ice concentrations—essentially a shift in the order of the EOFs and/or the spatial loadings—with no influence on the results presented here. Throughout this manuscript we use the term 'EOF pattern' to indicate the spatial fields derived from the analysis while the corresponding time series are referred to as 'principal components' (PC).

For temperature the updated instrumental series from Byrd Station by Monaghan et al. (2008) is used, having the advantage that it is located within the area spanned by those ITASE cores which show the strongest relationship to climate in all seasons (Sect. 3). Prior to 1998, the Byrd record remains the same as described by Monaghan et al. (2008), which we briefly summarize here. The authors used monthly mean temperature observations from the manned Byrd station record from January 1957 to September 1970. From October 1970 to December 1978, only a few scattered summer observations were available from the manned Byrd station record, and therefore the missing months for this period were infilled with temperatures estimated using multiple linear regression with other Antarctic manned station records. After 1979, an automatic weather station (Byrd AWS) was installed at the former manned station. From January 1979 through December 1997, missing Byrd AWS temperatures were infilled by Shuman and Stearns (2001, 2002) with a technique that employed satellite microwave brightness temperatures. Byrd AWS observations were available for 68 % of the months during this period, and thus 32 % of the months were infilled using the Shuman and Stearns technique.

Beginning in 1998, the missing monthly mean Byrd AWS temperature data have been infilled using temperature records from four nearby AWS stations, the first two of which were installed in 1994 (Suppl. Table 1). For a monthly mean to be considered valid, at least 70 % of the hourly measurements for a given month must be available. For months that have less than 70 % of measurements due to AWS outages, the Byrd AWS temperatures are estimated by equally weighting the adjusted temperature of each nearby AWS that has data available for a given month. The adjusted temperature for each of the contributing stations is calculated by adding the long-term (1995–2009) monthly average temperature difference between that station and Byrd AWS to the station record prior to weighting, thereby giving the effective temperature at Byrd AWS. For the twelve-year period from 1998 to 2009, the Byrd AWS observations are available for 64 % of the months, and therefore the weighted infilling was required for 36 % of the months. To test the accuracy of the infilling methodology, the seasonal averages of the weighted infilled Byrd AWS seasonal estimates were compared with the actual Byrd AWS data for the periods during which the Byrd AWS data were available (Suppl. Fig. 3). The infilled estimates agree closely with the values at Byrd AWS ($r^2 = 0.99$, $p < 0.001$, RMSE = 0.64 °C),

indicating that our methodology for infilling missing Byrd AWS data after 1998 is robust. This is further supported by comparing the updated Byrd AWS record with the Steig et al. (2009) temperature record at the grid box collocated with Byrd; the two records are very similar despite different methodologies.

## 3 Results

Figure 4 presents the annual means of the ITASE cores for the period 1900–1999, expressed as regional and overall averages of the eight cores. While the cores all show a similar multidecadal evolution, spatially distinct differences are found that relate to the position of the cores with respect to the WAIS Divide. As shown in the correlation matrix in Table 2, cores to the east and west of WAIS Divide, respectively, have statistically significant correlations only with the cores located within the same region of West Antarctica. The core 2000–1, located on the WAIS Divide, is the only core that shows significant correlations with cores from all parts of West Antarctica. This suggests that this location is representative for large parts of West Antarctica, which is of particular relevance for the interpretation and significance of the deep ice core (expected total age of about 100,000 years) recently drilled at WAIS Divide, about 22 km from ITASE core 2000–1.

In Table 2, and throughout the paper, correlation coefficients presented are based on linearly detrended data and tested with a two-tailed $t$ test, reducing the sample size $T$ according to the lag-1 autocorrelation of the data ($r_1$ and $r_2$; Bretherton et al. 1999):

$$T^* = T\frac{1 - r_1 r_2}{1 + r_1 r_2} \tag{5}$$

### 3.1 The strong 1980 anomaly

A distinctive feature of the annual average isotope records shown in Fig. 4 is the very strong $\delta$-anomaly found in the year 1980 (see also Fig. 3). This positive anomaly is particularly pronounced in the westernmost cores (2000–1, 2000–4, 2000–5), and there is a corresponding strong negative anomaly in the southernmost core (2002–4). Indeed, 1980 is the single largest positive anomaly on

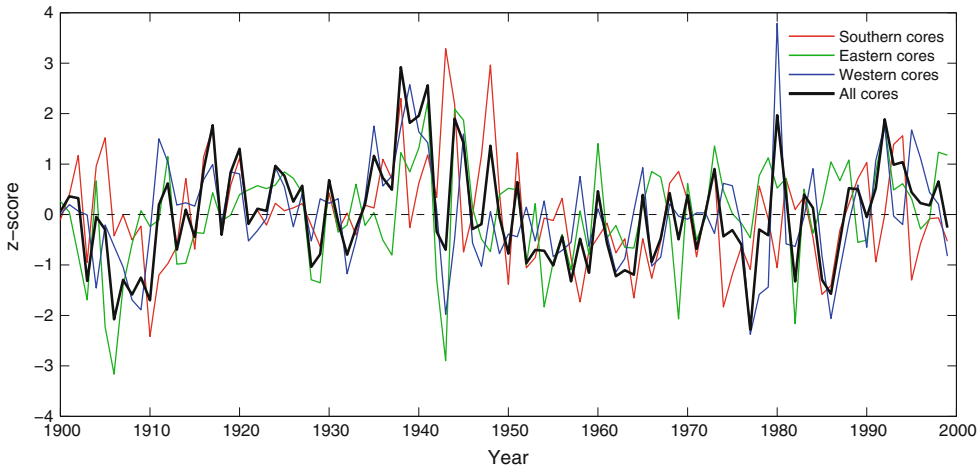


**Fig. 4** Standardized $\delta^{18}$O/$\delta$D annual means of the ITASE cores 1900–1999, expressed as regional averages. The *red line* is the mean of the southernmost cores (2001–2, 2002–2, 2002–4), the *green line* the mean of the easternmost cores (2001–3, 2001–5), and the *blue line* the mean of the westernmost cores (2000–1, 2000–4, 2000–5). The *thick black line* is the mean of all eight cores

**Table 2** Correlations of the annually averaged ITASE cores 1900–1999

| | Divide | West | | South | East | | South | |
|---|---|---|---|---|---|---|---|---|
| | 2000–1 | 2000–4 | 2000–5 | 2001–2 | 2001–3 | 2001–5 | 2002–2 | 2002–4 |
| 2000–1 | | **0.228** | **0.317** | −0.204 | **0.288** | **0.214** | 0.022 | −0.019 |
| 2000–4 | **0.228** | | **0.301** | −0.122 | 0.033 | 0.120 | 0.136 | −0.063 |
| 2000–5 | **0.317** | **0.301** | | −0.033 | 0.061 | 0.155 | 0.081 | 0.086 |
| 2001–2 | −0.204 | −0.122 | −0.033 | | −0.135 | −0.163 | 0.167 | **0.221** |
| 2001–3 | **0.288** | 0.033 | 0.061 | −0.135 | | **0.291** | 0.037 | 0.114 |
| 2001–5 | **0.214** | 0.120 | 0.155 | −0.163 | **0.291** | | −0.019 | 0.139 |
| 2002–2 | 0.022 | 0.136 | 0.081 | 0.167 | 0.037 | −0.019 | | 0.053 |
| 2002–4 | −0.019 | −0.063 | 0.086 | **0.221** | 0.114 | 0.139 | 0.053 | |

Significant values ($p \leq 0.05$) are underlined and in bold. The top row indicates the location within West Antarctica as shown in Fig. 1

record in the 2000–4 core, which is the westernmost core except for nearby 2000–5 (which also has a strong positive anomaly in 1980). The single largest negative anomaly in the 2002–4 core, which is the southernmost core, also occurs in 1980.

Besides the strong $\delta$-anomaly, a significant climatic event also occurs in 1980, and this year therefore offers a useful case study of the complex relationships between West Antarctic isotopic variations and regional sea ice, local temperature, and the large-scale atmospheric circulation: the smallest sea ice extent in the Ross Sea in the post-1979 satellite era (particularly in MAM; Comiso and Nishio 2008) is found in 1980, while a record high sea ice extent is concurrently found in the Weddell Sea (Cavalieri and Parkinson 2008); this is a clear example of the Antarctic Dipole introduced by Yuan and Martinson (2001). Furthermore, the second largest positive deviation of the first PC of annual mean, linearly detrended Southern Hemisphere (SH; <30°S) Z500 from both ERA40 (Uppala et al. 2005) and NCEP (Kalnay et al. 1996) for the time period 1957 through 2001 is found in 1980 and is related to a positive circulation anomaly centered over the Amundsen Sea. Additionally, Genthon et al. (2005) find a very strong positive (negative) surface mass balance anomaly in the westernmost (easternmost) part of West Antarctica in 1980, reflecting the moist onshore (dry offshore) winds prevailing in this year. Moreover, 1980 is the second warmest year since the record started in 1957 at Byrd Station (only 2007 is warmer), with MAM of 1980 being the overall warmest and JJA of 1980 being the overall second warmest year. Finally, the station-based SAM index of Marshall (2003) also shows strongly negative values during MAM of 1980.

Figure 5 shows the 1980 seasonal mean anomaly fields (with respect to the 1979–1999 mean) of HadISST Antarctic sea ice concentrations and ERA40 Z500 along with the seasonal mean z-scores of the ITASE $\delta$-profiles (standardized over the 1979–1999 period). The ITASE z-scores are represented by colored circles with the size reflecting the magnitude of the deviation. The z-values of the eight cores are given in the Table of Fig. 5. During austral summer (DJF), large $\delta$-anomalies are only found for the western- and southernmost cores, with the pronounced positive isotopic anomaly spreading eastward as the year advances. Peak anomalies in the majority of the cores, reaching up to 2.6 standard deviations, are found in austral fall (MAM) and winter (JJA) with, however, the largest anomalies in the easternmost core occurring in JJA and austral spring (SON). Remarkably, both the negative sea ice anomaly and the related strongly positive circulation anomaly also show an eastward movement from DJF to SON with the peak intensity as well being found in austral fall and winter. A similar, slightly stronger height anomaly is found in the upper levels of the atmosphere during 1980 (not shown), indicating an approximately equivalent barotropic vertical structure of the atmosphere, suggesting that the circulation anomaly is an atmospheric forcing of the sea ice rather than a response to the sea ice anomaly (Bretherton 1964; Hoskins and Karoly 1981).

The correspondence of above normal $\delta$ values in most ITASE cores with low sea ice concentrations in the adjacent ocean and anomalously high geopotential heights in 1980 (Fig. 5) presumably results from both the increased transport of high $\delta$ moisture from lower latitudes into West Antarctica and the anomalously large influx of fresh, isotopically less depleted, water vapor from the relatively ice free Southern Ocean. This is consistent with expectations from model simulations (e.g. Noone and Simmonds 2004). Additionally, there is an eastward seasonal propagation in the peak signal in the ITASE cores that is concurrent with the eastward propagation of the positive atmospheric circulation and the negative sea ice anomalies, which clearly shows that seasonal information can be extracted from the ITASE $\delta$ profiles. The year 1980 thus exemplifies the joint influence of atmospheric circulation and sea ice on West Antarctic isotopic compositions. However, this represents only a single year. In the next section, we consider whether the same relationships observed for 1980 can be found more generally on a longer time scale.

### 3.2 Long-term seasonal climate information preserved in the ITASE cores

We now compare the complete seasonal time series (1979–1999) of the ITASE cores with Antarctic sea ice concentrations, the large-scale atmospheric circulation, and temperature at Byrd Station. Significant correlations are generally found only for the westernmost sites, cores 2000–1, 2000–4, and 2000–5. This is an important finding, suggesting that the location of the ice core profiles is much more important than the snow accumulation rate, which is comparably low at these westernmost sites (Table 1). We accordingly next focus only on the results obtained for the three westernmost ITASE cores, using the first PC time series (hereafter referred to as ITASE PC 1) of the linearly detrended and standardized data. As for Z500 and sea ice, the ITASE EOFs are calculated for each 3-month period separately. The first EOF explains 55–65 % of the total variance of the three cores and the associated PC 1 is very similar to the simple average of these cores, with seasonal correlations ranging from 0.95 to 0.99. All three cores contribute significantly to ITASE PC 1 with, however, the westernmost cores (2000–4, 2000–5) having the largest weight in all seasons (Suppl. Fig. 4). We note that highly significant correlations ($p \leq 0.05$) between the three cores is found for all seasons and that the results presented here essentially also apply to the three individual cores. In the

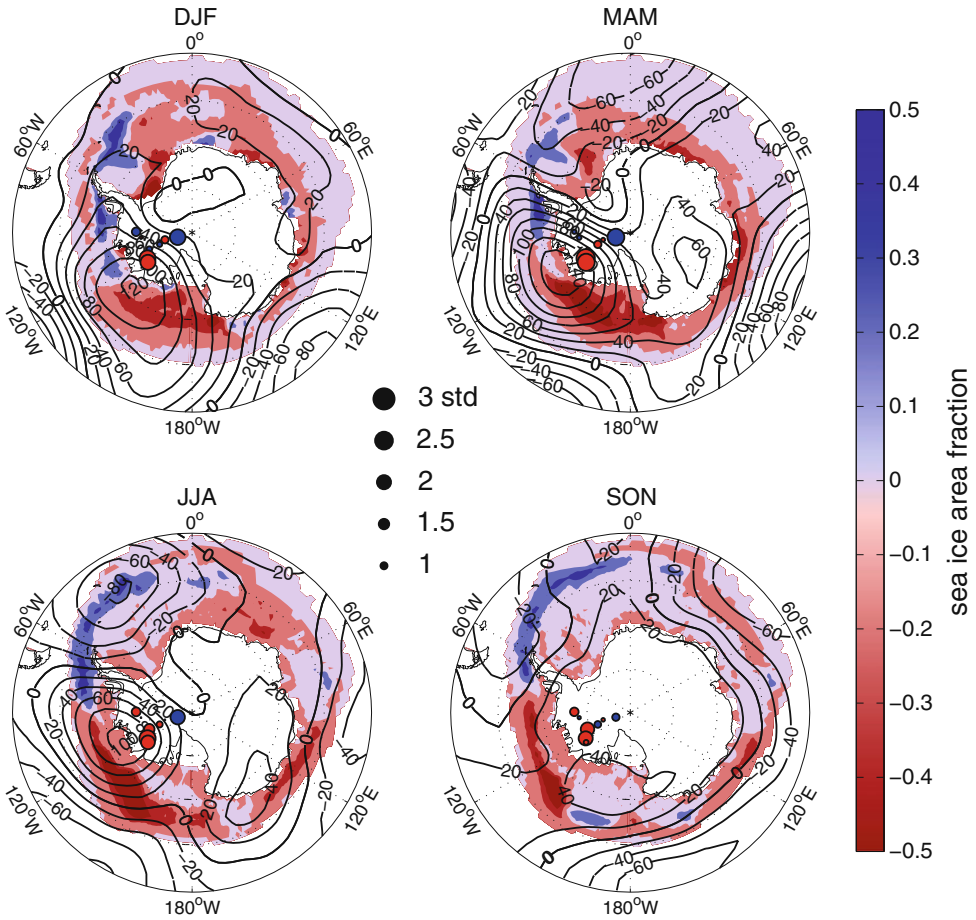


| | 2000-1 | 2000-4 | 2000-5 | 2001-2 | 2001-3 | 2001-5 | 2002-2 | 2002-4 |
|---|---|---|---|---|---|---|---|---|
| **DJF** | -0.816 | 2.257 | 2.125 | -0.766 | 0.415 | -1.236 | ***1.036*** | -2.217 |
| **MAM** | 0.436 | ***2.582*** | ***2.422*** | ***1.047*** | ***-0.665*** | -0.620 | 0.591 | ***-2.410*** |
| **JJA** | 1.487 | 2.283 | 1.964 | 0.883 | 0.165 | ***1.252*** | 0.169 | -2.031 |
| **SON** | ***1.935*** | 2.017 | 0.707 | -0.980 | -0.512 | 1.213 | 0.540 | -1.074 |

**Fig. 5** Seasonal $\delta^{18}O/\delta D$ z-scores (*blue* indicates negative, *red* positive deviations) of the ITASE cores along with the spatial anomalies (wrt 1979–1999) of HadISST Antarctic sea ice area fraction and ERA40 Z500 for the year 1980. The size of the *blue* and *red dots* in the four panels reflects the magnitude of the ITASE z-scores given in the table with the scale shown in the center of the four panels. *Bold* values in the table indicate the season with the largest z-score for each core

following, we present results based on the cores diffused to the equivalent of 1979. Diffusing these three ITASE cores to 1957, the results presented later for Byrd Station temperature and Z500 are also confirmed for the 1957–1999 period (not shown).

### 3.2.1 Regression of ITASE PC 1 against Z500 and sea ice

Figure 6 presents for the four conventionally defined seasons the regression of the standardized ITASE PC 1 against the Antarctic Z500 and sea ice fields. Significant correlations ($p \leq 0.05$) are depicted by the gray shaded areas (Z500) and the thick black contour lines (sea ice), respectively. In order to isolate the influence of the strong 1980 anomaly, the results are presented with and without including 1980 in the regression and correlation calculations. Comparison of these results with the 1980 event (Fig. 5) allows one to determine whether the spatial structure and amplitude of the atmospheric circulation and sea ice anomalies found in 1980 constitute a unique event or are rather a typical representation of the circulation and sea ice patterns that influence the seasonal isotopic variations in western West Antarctica.

The Z500 regression patterns derived with and without including 1980 (Fig. 6), are similar for all seasons except JJA. In both cases, statistically significant correlations over West Antarctica are found in DJF and MAM, and to a lesser degree in SON. For DJF (Fig. 6, top row), a positive anomaly in ITASE PC 1 is strongly related to a well developed positive circulation anomaly in the Ross and Amundsen Seas, with zonal wind anomalies dominating over West Antarctica. For MAM (Fig. 6, second row), a similarly strong positive Z500 anomaly is found which, however, is centered over West Antarctica (to the east of the DJF anomaly center) thus inducing predominantly meridional onshore winds towards western West Antarctica.

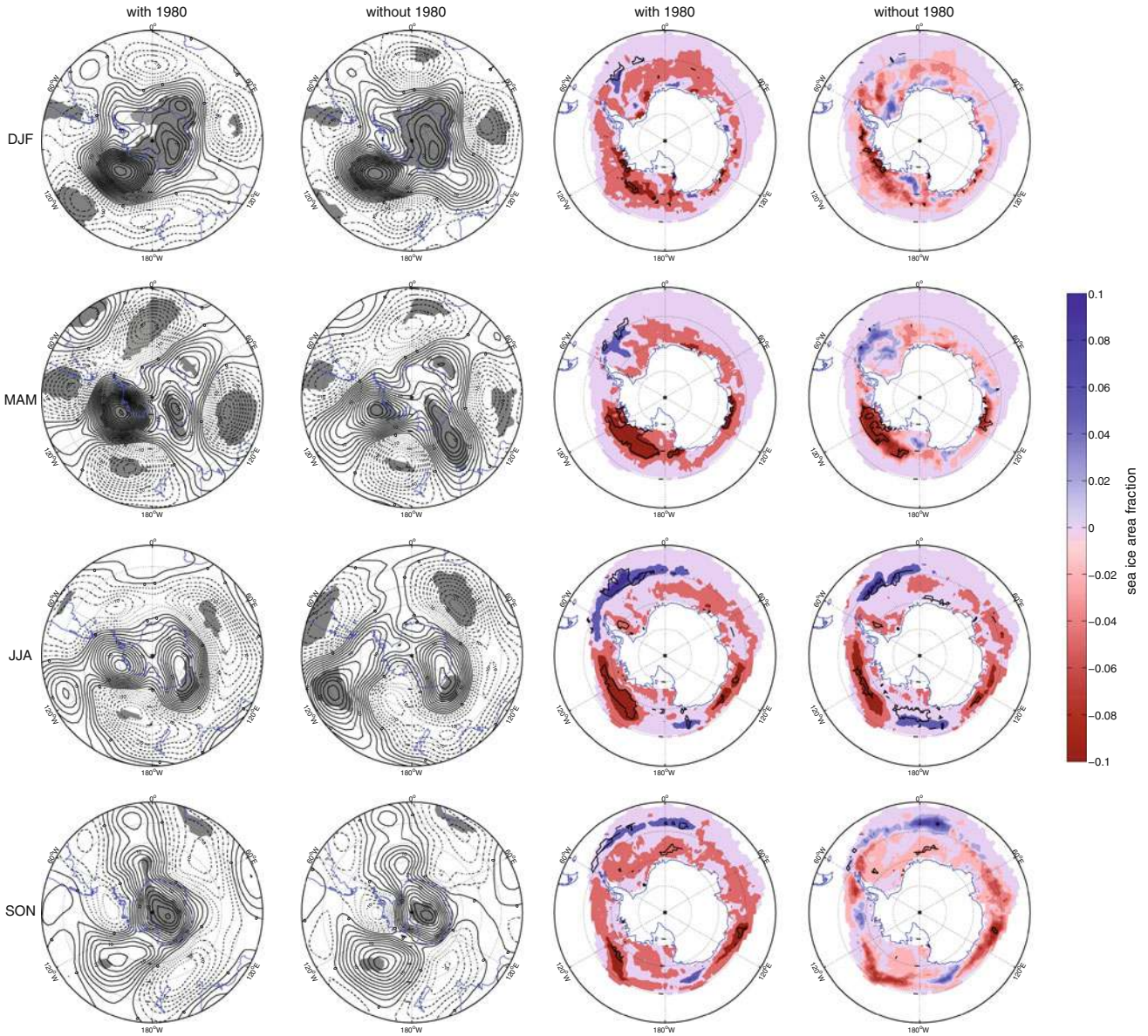


**Fig. 6** Regression of the standardized seasonal ITASE PC 1 against ERA40 Z500 (contour interval 2 m) and HadISST sea ice area fraction for the four conventionally defined seasons DJF, MAM, JJA, and SON 1979–1999. Areas with significant correlations ($p \leq 0.05$) are *shaded* in *gray* (Z500) and *encircled* by a *thick black contour line* (sea ice), respectively. 1980 is included in columns 1 and 3, while this year is excluded prior to correlation and regression in columns 2 and 4

For JJA (Fig. 6, third row), a similar pattern is found but it is not statistically significant; this positive circulation anomaly over West Antarctica is largely due to the inclusion of 1980. For SON (Fig. 6, bottom row), significant correlations between ITASE PC 1 and Z500 are found only for a positive circulation anomaly west of the Ross Sea. Similar results are found for sea ice, with again a small dependence on including or withholding 1980 (Fig. 6, columns 3 and 4): A very strong and highly significant negative correlation between ITASE PC 1 and sea ice in the Ross and Amundsen Seas is found in both MAM and JJA, with the significant area being closer to the West Antarctic coast in MAM. During these two seasons, the long-term relationship between ITASE PC 1 and sea ice agrees very well with the pattern found in 1980 (Fig. 5), while larger differences prevail for DJF and SON. These results therefore demonstrate that positive $\delta$-anomalies in the westernmost ITASE cores—as exemplified by 1980, but not limited to that single year—are generally related to strong, anomalously onshore winds towards these sites, and corresponding negative sea ice anomalies in the adjacent Ross and Amundsen Seas.

### 3.2.2 *Seasonal correlations between ITASE PC 1 and the dominant modes of Z500, sea ice, and near-surface air temperature*

Figure 6 demonstrates that the isotopic composition of the westernmost ITASE cores shows seasonally distinct patterns in the relationship to the large-scale atmospheric circulation and sea ice. These spatial regression patterns are very similar to the dominant modes (EOF 1) of the atmospheric circulation and sea ice (Suppl. Fig. 5). Accordingly, we next investigate how ITASE PC 1 is related to the seasonally dominating modes of circulation and sea ice, as well as to temperature at Byrd Station over the period 1979–1999. As shown in Fig. 6, ITASE PC 1 is significantly related to the circumpolar Z500 field while significant correlations with sea ice are mainly found for the Pacific Sector of West Antarctica. Accordingly, the entire SH south of 30°S is used for the calculation of the Z500 EOFs while the limited area of 180°–70°W is used for sea ice. The results presented next are maintained when considering the entire SH for sea ice.

Figure 7 (left panels) shows correlation coefficients between ITASE PC 1 and the first PC of SH Z500, the first PC of West Antarctic sea ice concentrations, and temperature at Byrd Station for three month averages (see also Supp. Fig. 2). The corresponding EOF patterns are found in Supplementary Fig. 4. Note that positive correlations in Fig. 7 mean for all seasons that above normal $\delta$-values are generally related to enhanced meridional onshore flow towards western West Antarctica, less sea ice in the Ross and Amundsen Seas, and warmer temperatures at Byrd Station. As already shown in Fig. 6, the correlations depend to some extent on 1980, being of no surprise considering the strong anomaly found in this year. However, the seasonal evolution of the correlations is not importantly altered by excluding 1980 (blue lines in Fig. 7): Statistically significant ($p \leq 0.05$) positive correlations between ITASE PC 1 and Z500 PC 1 are found for austral summer

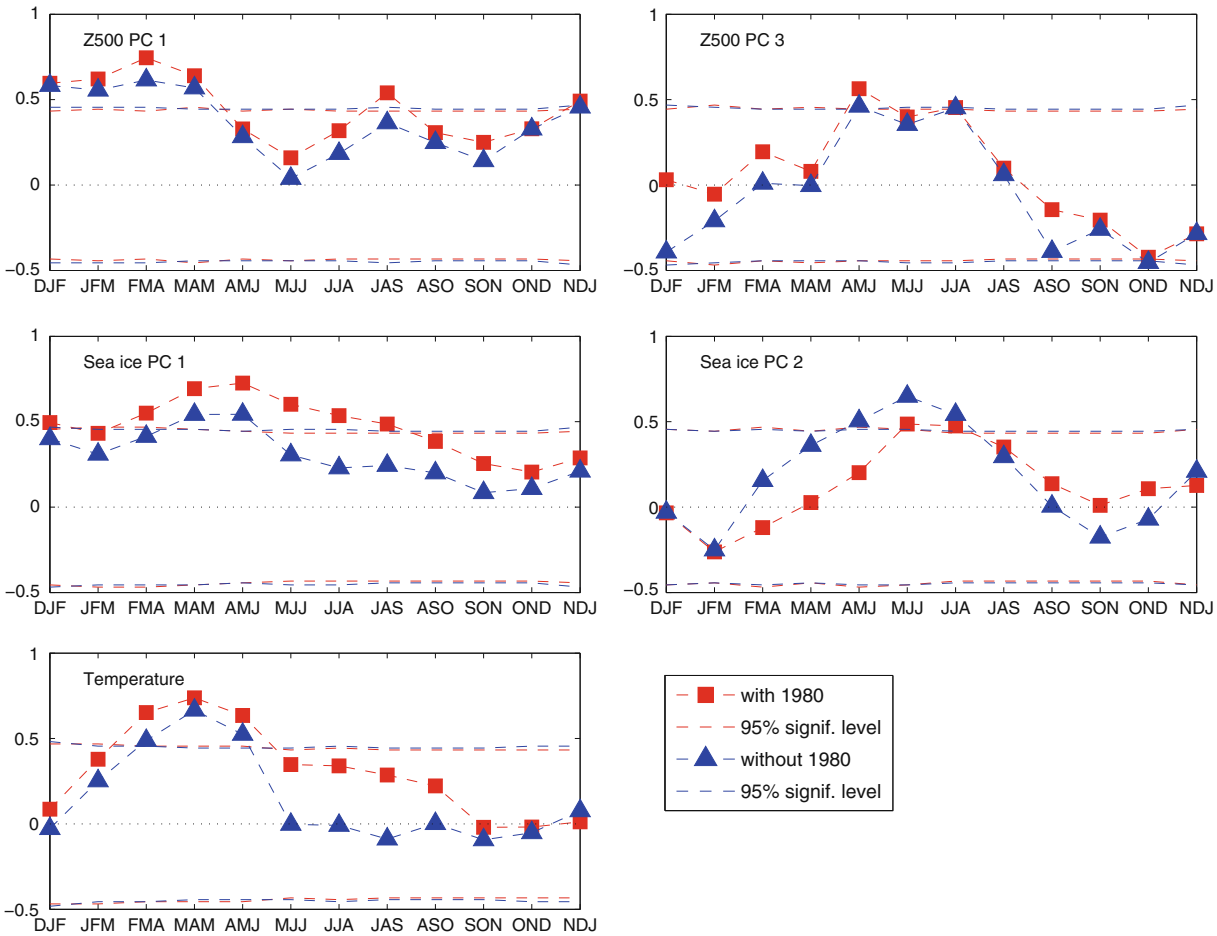


**Fig. 7** Correlation coefficients between ITASE PC 1 and the first (*top left panel*) and third (*top right panel*) PC of ERA40 Z500 south of 30°S, the first (*middle left panel*) and second (*middle right panel*) PC of HadISST West Antarctic [180°–70°W] sea ice area fraction, and temperature at Byrd Station (*bottom left panel*) for 3-month averages 1979–1999. The *red line* (*squares*) includes 1980 while this year is withheld in the *blue line* (*triangles*). The *dashed quasi-horizontal red* and *blue lines* indicate the 95 % significance levels

and fall (Fig. 7, top left panel), demonstrating that ITASE PC 1 during this part of the year is strongly linked to the dominant mode of the large-scale atmospheric circulation. For sea ice (Fig. 7, middle left panel) and temperature (bottom left panel), a seasonal evolution of the correlation coefficients similar to Z500 is found but with the peak correlations in both pairs occurring in fall. These results are in very good agreement with the results presented in Fig. 6. The slope found between $\delta$ and temperatures during fall ($\sim$0.4 ‰/K) compares well with previous work, showing typical slopes of $\sim$0.5–0.8 ‰/ °C for annual-mean correlations (Schneider et al. 2005; Masson-Delmotte et al. 2008; Fegyveresi et al. 2011). We note that significant correlations between ITASE PC 1 and Byrd temperatures are maintained when using precipitation-weighted temperatures (Supp. Fig. 6). The results shown in (Fig. 7) are also maintained when only using the higher accumulation cores 2000–1 and 2000–4 to construct ITASE PC 1 (Supp. Fig. 7), though the time of significant correlation is more narrowly restricted to austral fall only.

While no significant correlations between ITASE PC 1 and the first PC of sea ice and Z500 as well as temperature are found for austral winter, significantly positive correlations for this season are observed for the pairs of ITASE PC 1 and the third PC of Z500 (Fig. 7, top right panel) as well as the second PC of sea ice (Fig. 7, middle right panel). Again, these correlations are maintained if core 2000-5 is excluded, that is when only the two highest-accumulation rate cores are used to construct ITASE PC 1 (Supp. Fig. 7). The corresponding EOF patterns are found in Supplementary Fig. 8. Note that no significant seasonal correlations are found for the second EOF of Z500 or the third EOF of sea ice. While lower-order EOFs should always be interpreted with caution, the significantly positive ($p \leq 0.05$) correlations found in winter seem reasonable, indicating that positive $\delta$-anomalies are related to a negative circulation anomaly over the Ross Sea, directing anomalously onshore flow towards western West Antarctica, while, correspondingly, negative sea ice anomalies are evident in the Amundsen and Bellingshausen Seas (Suppl. Fig. 8). This also agrees with Supplementary Fig. 5 which shows that the Z500 regression pattern related to ITASE PC 1 during austral winter (Fig. 6) is equally highly correlated with the first as well third EOF of winter Z500 while the correlation of the West Antarctic sea ice regression pattern with the second EOF of sea ice is highest in winter.

It therefore appears that isotopic variations in western West Antarctica show a seasonally distinct relationship to

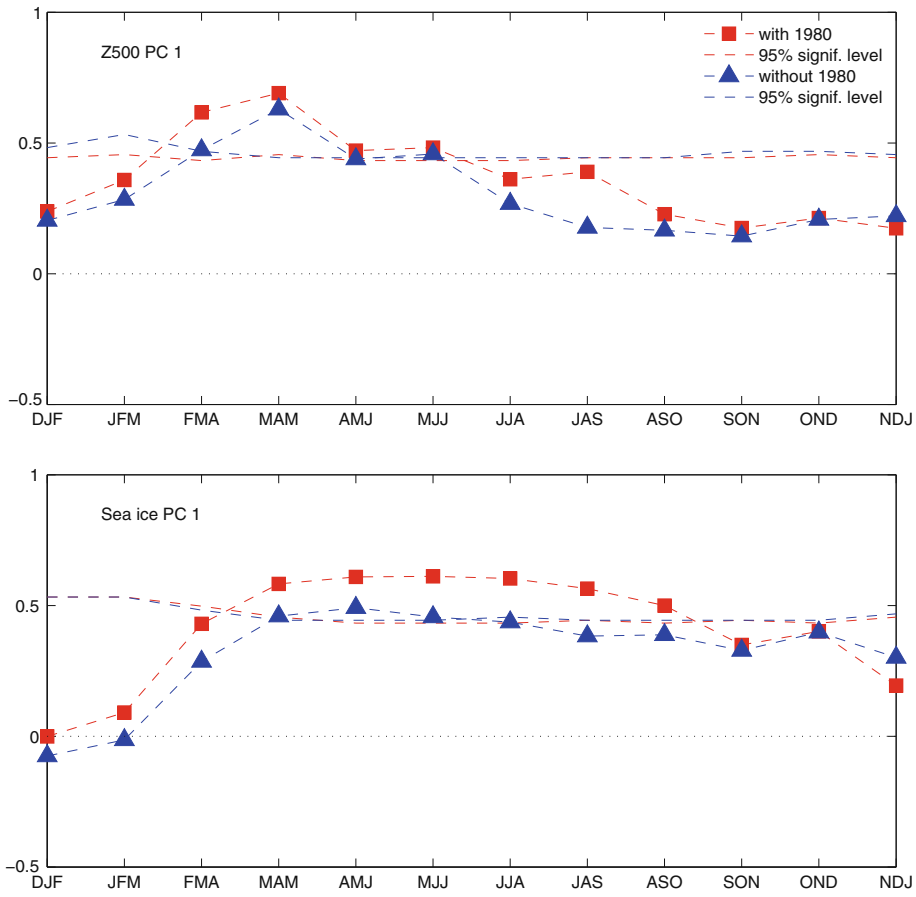


**Fig. 8** Correlation coefficients between temperature at Byrd Station and the first PC of ERA40 Z500 south of 30°S (*top panel*) as well as the first PC of HadISST West Antarctic [180°–70°W] sea ice area fraction (*bottom panel*) for 3-month averages 1979–1999. The *red line* (*squares*) includes 1980 while this year is withheld in the *blue line* (*triangles*). The *dashed quasi-horizontal red* and *blue lines* indicate the 95 % significance levels

the leading pattern of seasonal climate variability, with high and significant correlations with Z500 in austral summer, fall and winter, with sea ice in fall and winter, and with near-surface temperature at Byrd Station in fall only.

### 3.3 Seasonal correlations between Byrd Station temperature and the dominant modes of Z500 and sea ice

With $\delta$-variations often being used as a proxy for temperature, it is of interest to see whether the correlation patterns found in Fig. 7 are also observed for temperature. We therefore perform a similar analysis for temperature at Byrd Station, correlating it with the first PCs of Z500 and sea ice (Fig. 8). For sea ice, an evolution of the seasonal correlation with temperature very similar to the one obtained for ITASE PC 1 is found, both peaking in austral fall with lowest values in summer. Unlike for the PC 1 of the ITASE data, high and statistically significant correlations between temperature and Z500 are limited to austral fall and early winter. Again, excluding 1980 prior to correlation does not appreciably alter the results (blue lines in Fig. 8), with significant ($p \leq 0.05$) values still being obtained for austral fall and early winter. These results are in excellent agreement with Fig. 7, demonstrating that there is a strong relationship in fall between stable isotopes/surface temperatures in western West Antarctic and the state of the large-scale atmospheric circulation as well as offshore sea ice concentrations. With the highest correlation between ITASE PC 1 and Byrd Station temperature also being found in fall, it is evident that it is this season where the various factors influencing isotopic compositions go hand-in-hand. Next, we briefly explore why the climate signal may be particularly pronounced in austral fall.

### 3.4 Why is the large-scale climatic signal in the western ITASE cores primarily found in austral fall?

Fall is the season in which Antarctic sea ice is starting to grow, reaching peak concentrations off West Antarctica at the end of winter (September; e.g. Zwally et al. 2002). The variability in seasonally averaged sea ice concentrations off West Antarctica is also greatest in fall (Fig. 9, top panel). This illustrates that sea ice in this region is most dynamic during fall, which is also supported by the fact that month-to-month sea ice growth rates are largest from March to April with the average sea ice concentration increasing by $\sim$15 % (not shown). Averaging the monthly mean v-wind component over western West Antarctica (Fig. 9, bottom panel) reveals that the climatological meridional wind component directed towards western West Antarctica is strongest in austral fall, peaking in May. It therefore appears that the seasonally prevailing meridionally oriented atmospheric circulation, linked to rapidly changing sea ice concentrations offshore, results in a significant and

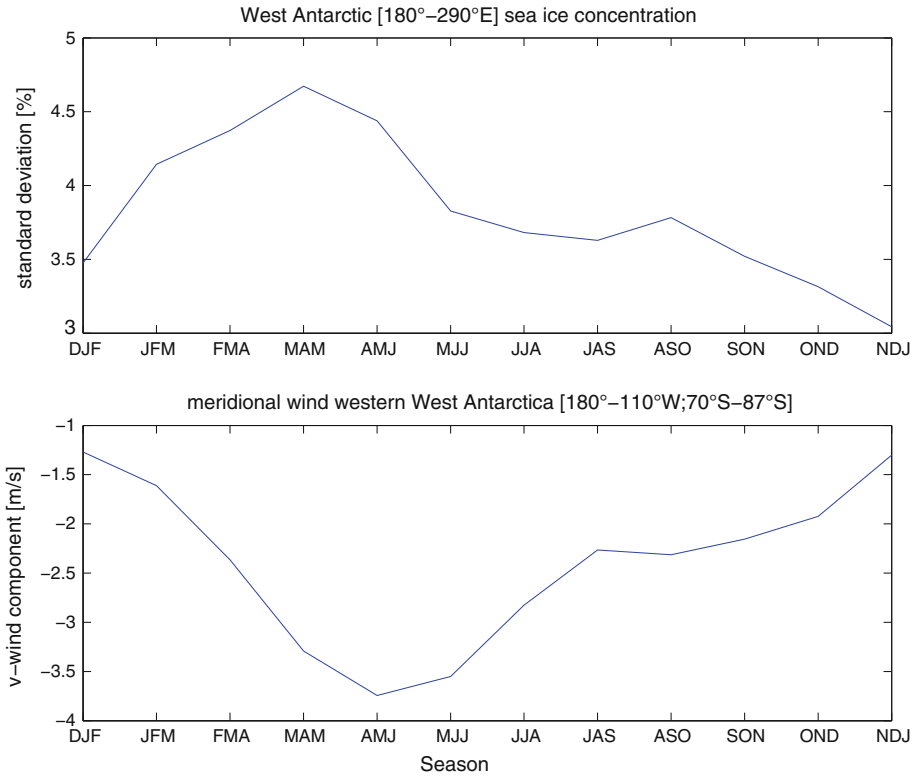


**Fig. 9** Standard deviation of average HadISST West Antarctic sea ice concentrations 1979–1999 [180°–110°W] (*top panel*) and seasonal average ERA40 Z500 v-wind component over western West Antarctica [180°–110°W; 70°S–87°S] 1979–1999 (*bottom panel*). The more negative the values of the v-wind component the stronger the northerly winds directed towards western West Antarctica

detectable large-scale climatic signal in the stable isotopic composition of West Antarctic precipitation during austral fall.

## 4 Discussion and conclusions

The results presented here demonstrate that sub-annual $\delta$-information can be successfully extracted from the ITASE cores. While sub-annual isotopic variations have been derived from other parts of Antarctica (e.g. Morgan and Van Ommen 1997), this study represents the first analysis of such data from West Antarctica. Although sub-annual information is mostly restricted to the mid-20th century due to the increasing effect of diffusion (Fig. 2), this time span overlaps the instrumental era and thus allows investigations of the factors dominating seasonal variations in West Antarctic water isotopic records.

As found in earlier studies (e.g. Fisher et al. 1985; Schneider et al. 2005; Vinther et al. 2010), we emphasize that using a network of ice core profiles is important for minimizing the influence of local noise inherent to single locations. Furthermore, the spatially extensive network of ITASE cores allows detailed investigations of isotopic variations across the pronounced topography of West Antarctica. As was reported in studies using $\delta$ and accumulation records from the ITASE dataset (Kaspari et al. 2004; Genthon et al. 2005; Schneider et al. 2005; Gregory and Noone 2008), spatially distinct differences in inter-core correlations and in the relationship to various climate variables are evident: the clearest climatic signal is obtained for the cores located on and west of the WAIS Divide. While the eastern ITASE cores may also contain important climatic information (e.g. Gregory and Noone 2008), the western sites are more readily interpretable, suggesting that these locations are more favorable for climate studies, even though the relatively low accumulation rates might initially suggest otherwise. Genthon et al. (2005) also report that only the surface mass balance at the ITASE cores located in the western part of West Antarctica have any discernible relationship to standard indices of large-scale climate variability such as the SAM and the Southern Oscillation. Referring to Genthon et al. (2003) they suggest that these spatial differences are due to the fact that the eastern ITASE cores are situated in the transition area where the correlation between the surface mass balance and the strength of the Amundsen Sea Low switches its sign. This means that the western ITASE cores are more optimally located with respect to the position of the Amundsen Sea Low, primarily receiving moisture from meridional winds. In contrast, the eastern ITASE cores are influenced by more variable wind directions, possibly also receiving significant portions of their moisture from the Weddell Sea. These eastern cores therefore not only receive moisture along more variable transportation paths than the western ones but possibly also from different source regions (see also Delaygue et al. 2000). Back trajectory analysis (e.g. Thomas and Bracegirdle 2009; Sodemann and Stohl 2009) may help to gain additional insights into the origin of these spatial differences.

Our results demonstrate that isotopic variations in the westernmost ITASE cores are strongly linked to the state of the large-scale atmospheric circulation, sea ice concentrations offshore, as well as local temperatures. However, distinct seasonal differences prevail: While significant correlations of the isotope data with the circulation over West Antarctica are also found for austral summer and winter, and with sea ice in winter, it is only during austral fall that significant correlations are found with all three climate variables: large-scale atmospheric circulation, West Antarctic sea ice, and temperature. Notably, a very similar seasonal evolution of the correlation coefficients is observed between the instrumental temperature at Byrd Station and the dominant circulation as well as sea ice patterns, both pairs peaking and only being significant in austral fall and early winter. Our analysis suggests that this seasonally distinct pattern can be related to the leading pattern of atmospheric variability, which has a direct impact on temperature in West Antarctica and a direct impact on sea ice concentration offshore. The latter anomalies contribute greatly to the isotope records in West Antarctica because the climatological wind during this season has a strong onshore (meridional) component (referred to as the wavenumber three pattern in Raphael 2007). Hence, in the fall season, the leading pattern of atmospheric variability drives anomalies in sea ice extent which, in turn, affect the relative fraction of (lighter) tropical vapor and (heavier) local vapor that is transported to West Antarctica and deposited in the form of snow. During the remainder of the year, the winds in the vicinity of West Antarctica are more zonally oriented and, as shown in Yuan and Li (2008), have generally a weaker influence on sea ice variations. In this context, the year 1980 where strong onshore winds, record-low sea ice concentrations and above-normal temperatures linked to the record-high positive isotopic anomaly prevail throughout the year, might be understood as the characteristic austral fall pattern.

With the highest correlations between sea ice concentrations and both the ITASE PC 1 and Byrd temperature being observed in fall, it might be speculated that the $\delta$-variations, rather than representing temperature itself, are actually reflecting sea ice variations offshore and therefore the distance to the source region, as e.g. suggested by Bromwich and Weaver (1983), Kato (1978), and Noone and Simmonds (2004). However, the fact that significant

correlations between $\delta$ and sea ice are predominantly found in fall rather suggests that both temperature and $\delta$ are particularly during this season strongly influenced by sea ice variations which themselves appear to be strongly driven by atmospheric circulation. This important point should however be investigated in much more detail in future studies e.g. by using climate model simulations which include a representation of stable isotopes (e.g. Hoffmann et al. 1998; Noone and Simmonds 2004). It would be particularly informative to use model simulations to quantify the relative magnitude of the contributions of the large-scale atmospheric circulation, sea ice, and temperature on the isotopic composition of West Antarctic precipitation, including considerations of time leads and lags.

Finally, we note that due to increasing diffusion and compaction with depth, $\delta$-records from West Antarctica extending past the $\sim$1950s will generally be interpretable only at annual or lower resolution. It is therefore of interest to consider the impact of seasonally variable relationships to the overall, annual isotope signal. Using the same three (westernmost) ITASE cores at annual resolution and extracting the first PC, we find a highly significant correlation of $r = 0.586$ ($p \leq 0.01$) with annual mean temperatures at Byrd Station over the 1979–1999 period ($r = 0.481$, $p \leq 0.01$ for 1957–1999). A similar or even slightly higher correlation is found between the first PC of annual mean isotopic composition in the westernmost cores and early austral fall (FMA) temperature at Byrd Station ($r = 0.622$ 1979–1999; $r = 0.477$ 1957–1999, both $p \leq 0.01$). This seasonal bias may be explained by the fact that both the $\delta$ variance of the seasonally resolved westernmost ITASE cores and of the temperature at Byrd Station peak in austral fall through late winter (Suppl. Fig. 9). Vinther et al. (2010) suggest a similar explanation for Greenland ice core isotope records. Additionally, austral fall through late winter $\delta$ and temperatures are highly ($r = 0.6$ to $r = 0.9$) correlated with annual mean $\delta$ and temperature, respectively (Suppl. Fig. 9). It therefore appears that both the annual average isotopic composition and annual average temperature in western West Antarctica are dominated by conditions in fall and winter. This is an important finding which has to be considered when interpreting isotopic records from this region.

**Acknowledgments** We thank University of Washington IsoLab staff and students A. Schauer, J. Flaherty, D. Schneider, P. Neff, K. Samek, R. Teel, and J. Bautista for help with the analyses. P. Mayewski and D. Dixon's coordination of the U.S. ITASE fieldwork was invaluable. This work was supported by grants OPP-0837988 and 0963924 from the National Science Foundation. The National Center for Atmospheric Research is funded by the National Science Foundation.

## References

Bretherton F (1964) Low frequency oscillations trapped near equator. Tellus 16:181–185

Bretherton C, Widmann M, Dymnikov V, Wallace J, Blade I (1999) The effective number of spatial degrees of freedom of a time-varying field. J Clim 12:1990–2009

Bromwich D, Weaver C (1983) Latitudinal displacement from main moisture source controls $\delta^{18}$O of snow in coastal Antarctica. Nature 301:145–147

Bromwich D, Guo Z, Bai L, Chen Q (2004) Modeled Antarctic precipitation part I: spatial and temporal variability. J Clim 17:427–447

Cavalieri D, Parkinson C (1981) Large-scale variations in observed Antarctic sea ice extent and associated atmospheric circulation. Mon Wea Rev 109:2323–2336

Cavalieri D, Parkinson CL (2008) Antarctic sea ice variability and trends, 1979–2006. J Geophys Res-Oceans 113:C07004. doi:10.1029/2007JC004564

Chapman WL, Walsh JE (2007) A synthesis of Antarctic temperatures. J Clim 20:4096–4117

Comiso JC, Nishio F (2008) Trends in the sea ice cover using enhanced and compatible AMSR-E, SSM/I, and SMMR data. J Geophys Res Oceans 113:C02S07. doi:10.1029/2007JC004257

Cuffey K, Steig E (1998) Isotopic diffusion in polar firn: implications for interpretation of seasonal climate parameters in ice-core records, with emphasis on central Greenland. J Glaciol 44:273–284

Dansgaard W (1964) Stable isotopes in precipitation. Tellus 16:436–468

Delaygue G, Masson V, Jouzel J, Koster RD, Healy RJ (2000) The origin of Antarctic precipitation: a modelling approach. Tellus 52:19–36

Ding QH, Steig EJ, Battisti DS, Küttel M (2011) Recent West Antarctic warming caused by central tropical Pacific warming. Nature Geosci 4:398–403

Divine DV, Isaksson E, Kaczmarska M, Godtliebsen F, Oerter H, Schlosser E, Johnsen SJ, van den Broeke M, van de Wal RSW (2009) Tropical Pacific-high latitude south Atlantic teleconnections as seen in $\delta^{18}$O variability in Antarctic coastal ice cores. J Geophys Res Atmos 114:D11112. doi:10.1029/2008JD010475

Dixon D, Mayewski P, Kaspari S, Sneed S, Handley M (2004) A 200 year sub-annual record of sulfate in West Antarctica, from 16 ice cores. Ann Glaciol 39:545–556

Epstein S, Sharp R, Goddard I (1963) Oxygen-isotope ratios in Antarctic snow, firn, and ice. J Geol 71:698–720

Fegyveresi JG, Alley RB, Spencer MK, Fitzpatrick JJ, Steig EJ, White JWC, McConnell JR, Taylor KC (2011) Late Holocen climate evolution at the WAIS Divide site, West Antarctica: bubble number-density estimate. J Glaciol 57:629–638

Fisher DA, Reeh N, Clausen HB (1985) Stratigraphic noise in time series derived from ice cores. Ann Glaciol 7:76–83

Genthon C, Krinner G, Sacchettini M (2003) Interannual Antarctic tropospheric circulation and precipitation variability. Clim Dyn 21:289–307

Genthon C, Kaspari S, Mayewski P (2005) Interannual variability of the surface mass balance of West Antarctica from ITASE cores and ERA40 reanalyses, 1958–2000. Clim Dyn 24:759–770

Gregory S, Noone D (2008) Variability in the teleconnection between the El Nino-Southern Oscillation and West Antarctic climate deduced from West Antarctic ice core isotope records. J Geophys Res Atmos 113:D17110. doi:10.1029/2007JD009107

Grootes P, Stuiver M (1986) Ross ice shelf oxygen isotopes and West Antarctic climate history. Quat Res 26:49–67

Hoffmann G, Werner M, Heimann M (1998) Water isotope module of the ECHAM atmospheric general circulation model: a study on timescales from days to several years. J Geophys Res Atmos 103:16871–16896

Hoskins B, Karoly D (1981) The steady linear response of a spherical atmosphere to thermal and orographic forcing. J Atmos Sci 38:1179–1196

Johnsen SJ (1977) Stable isotope profiles compared with temperature profiles in firn and with historical temperature records. Proceedings of symposium on isotopes and impurities in snow and ice, Grenoble Aug–Sept 1975. Int Ass Hydrol Sci Publ 118:388–392

Johnsen SJ, Clausen HB, Cuffey KM, Hoffmann G, Schwander J, Creyts T (2000) Diffusion of stable isotopes in polar firn and ice: the isotope effect in firn diffusion. In: Hondoh T (ed) Physics of ice core records. Hokkaido University Press, Sapporo, pp 121–140

Kalnay E, Kanamitsu M, Kistler R, Collins W, Deaven D, Gandin L, Iredell M, Saha S, White G, Woollen J, Zhu Y, Chelliah M, Ebisuzaki W, Higgins W, Janowiak J, Mo K, Ropelewski C, Wang J, Leetmaa A, Reynolds R, Jenne R, Joseph D (1996) The NCEP/NCAR 40-year reanalysis project. Bull Am Meteorol Soc 77:437–471

Kaspari S, Mayewski P, Dixon D, Spikes V, Sneed S, Handley M, Hamilton G (2004) Climate variability in West Antarctica derived from annual accumulation-rate records from ITASE firn/ice cores. Ann Glaciol 39:585–594

Kato K (1978) Factors controlling oxygen isotopic composition of fallen snow in Antarctica. Nature 272:46–48

Marshall GJ (2003) Trends in the southern annular mode from observations and reanalyses. J Clim 16:4134–4143

Masson-Delmotte V, Hou S, Ekaykin A, Jouzel J, Aristarain A, Bernardo RT, Bromwich D, Cattani O, Delmotte M, Falourd S, Frezzotti M, Gallee H, Genoni L, Isaksson E, Landais A, Helsen MM, Hoffmann G, Lopez J, Morgan V, Motoyama H, Noone D, Oerter H, Petit JR, Royer A, Uemura R, Schmidt GA, Schlosser E, Simoes JC, Steig EJ, Stenni B, Stievenard M, van den Broeke MR, van de Wal RSW, van de Berg WJ, Vimeux F, White JWC (2008) A review of Antarctic surface snow isotopic composition: observations, atmospheric circulation, and isotopic modeling. J Clim 21:3359–3387

Mayewski PA, Frezzotti M, Bertler N, Van Ommen T, Hamilton G, Jacka TH, Welch B, Frey M, Qin D, Ren J, Simoes J, Fily M, Oerter H, Nishio F, Isaksson E, Mulvaney R, Holmund P, Lipenkov V, Goodwin I (2005) The international trans-antarctic scientific expedition (ITASE): an overview. Ann Glaciol 41:180–185

Mo KC, Ghil M (1987) Statistics and dynamics of persistent anomalies. J Atmos Sci 44:877–901

Monaghan AJ, Bromwich DH, Chapman W, Comiso JC (2008) Recent variability and trends of Antarctic near-surface temperature. J Geophys Res Atmos 113:D04105. doi:10.1029/2007JD009094

Morgan V, van Ommen T (1997) Seasonality in late-Holocene climate from ice-core records. Holocence 7:351–354

Nicolas JP, Bromwich DH (2011) Climate of West Antarctica and influence of marine air intrusions. J Clim 24:49–67

Noone D, Simmonds I (2002a) Associations between $\delta$18O of water and climate parameters in a simulation of atmospheric circulation for 1979–1995. J Clim 15:3150–3169

Noone D, Simmonds I (2002b) Annular variations in moisture transport mechanisms and the abundance of $\delta^{18}$O in Antarctic snow. J Geophys Res Atmos 107:4742. doi:10.1029/2002JD002262

Noone D, Simmonds I (2004) Sea ice control of water isotope transport to Antarctica and implications for ice core interpretation. J Geophys Res Atmos 109:D07105. doi:10.1029/2003JD004228

Raphael MN (2007) The influence of atmospheric zonal wave three on Antarctic sea ice variability. J Geophys Res Atmos 112:D12112. doi:10.1029/2006JD007852

Rayner N, Parker D, Horton E, Folland C, Alexander L, Rowell D, Kent E, Kaplan A (2003) Global analyses of sea surface temperature, sea ice, and night marine air temperature since the late nineteenth century. J Geophys Res Atmos 108:4407. doi:10.1029/2002JD002670

Scheider DP, Steig EJ, Comiso JC (2004) Recent climate variability in Antarctica from satellite-derived temperature data. J Clim 17:1569–1583

Schneider DP, Noone DC (2007) Spatial covariance of water isotope records in a global network of ice cores spanning twentieth-century climate change. J Geophys Res Atmos 112:D18105. doi:10.1029/2007JD008652

Schneider DP, Steig EJ (2008) Ice cores record significant 1940 s Antarctic warmth related to tropical climate variability. Proc Natl Acad Sci 105:12154–12158

Schneider DP, Steig EJ, van Ommen T (2005) High-resolution ice-core stable-isotopic records from Antarctica: towards interannual climate reconstruction. Ann Glaciol 41:63–70

Schneider DP, Deser C, Okumura Y (2012) An assessment and interpretation of the observed warming of West Antarctica in the austral spring. Clim Dyn 38:323–347. doi:10.1007/s00382-010-0985-x

Shuman CA, Stearns CR (2001) Decadal-length composite inland West Antarctic temperature records. J Clim 14:1977–1988

Shuman CA, Stearns CR (2002) Decadal-length composite West Antarctic air temperature records. National Snow and Ice Data Center, Digital media, Boulder, CO

Sime LC, Wolff EW, Oliver KIC, Tindall JC (2009) Evidence for warmer interglacials in East Antarctic ice cores. Nature 462:342–345

Sodemann H, Stohl A (2009) Asymmetries in the moisture origin of Antarctic precipitation. Geophys Res Lett 36:L22803. doi:10.1029/2009GL040242

Stammerjohn SE, Martinson DG, Smith RC, Yuan X, Rind D (2008) Trends in Antarctic annual sea ice retreat and advance and their relation to El Nino-Southern Oscillation and Southern Annular Mode variability. J Geophys Res Oceans 113:C03S90. doi:10.1029/2007JC004269

Steig EJ (2009) US ITASE Stable isotope data, Antarctica. National Snow and Ice Data Center. DIF: NSIDC-0425

Steig EJ, Mayewski PA, Dixon DA, Kaspari SD, Frey MM, Schneider DP, Arcone SA, Hamilton GS, Spikes VB, Albert M, Meese D, Gow AJ, Shuman CA, White JWC, Sneed S, Flaherty J, Wumkes M (2005) High-resolution ice cores from US ITASE (West Antarctica): development and validation of chronologies and determination of precision and accuracy. Ann Glaciol 41:77–84

Steig EJ, Schneider DP, Rutherford SD, Mann ME, Comiso JC, Shindell DT (2009) Warming of the Antarctic ice-sheet surface since the 1957 International Geophysical Year. Nature 457:459–462

Thomas ER, Bracegirdle TJ (2009) Improving ice core interpretation using in situ and reanalysis data. J Geophys Res Atmos 114:D20116. doi:10.1029/2009JD012263

Torrence C, Compo G (1998) A practical guide to wavelet analysis. Bull Am Meteorol Soc 79:61–78

Turner J, Comiso JC, Marshall GJ, Lachlan-Cope TA, Bracegirdle T, Maksym T, Meredith MP, Wang Z, Orr A (2009) Non-annular atmospheric circulation change induced by stratospheric ozone depletion and its role in the recent increase of Antarctic sea ice extent. Geophys Res Lett 36:L08502. doi:10.1029/2009GL037524

Uppala S, Kallberg P, Simmons A, Andrae U, Bechtold V, Fiorino M, Gibson J, Haseler J, Hernandez A, Kelly G, Li X, Onogi K, Saarinen S, Sokka N, Allan R, Andersson E, Arpe K, Balmaseda M, Beljaars A, Van De Berg L, Bidlot J, Bormann N, Caires S, Chevallier F, Dethof A, Dragosavac M, Fisher M, Fuentes M,

Hagemann S, Holm E, Hoskins B, Isaksen L, Janssen P, Jenne R, McNally A, Mahfouf J, Morcrette J, Rayner N, Saunders R, Simon P, Sterl A, Trenberth K, Untch A, Vasiljevic D, Viterbo P, Woollen J (2005) The ERA-40 re-analysis. Quart J Roy Meteor Soc 131:2961–3012

Vinther BM, Jones PD, Briffa KR, Clausen HB, Andersen KK, Dahl-Jensen D, Johnsen SJ (2010) Climatic signals in multiple highly resolved stable isotope records from Greenland. Quat Sci Rev 29:522–538

White WB, Peterson RG (1996) An Antarctic circumpolar wave in surface pressure, wind, temperature and sea-ice extent. Nature 380:699–702

Yuan X, Li C (2008) Climate modes in southern high latitudes and their impacts on Antarctic sea ice. J Geophys Res Oceans 113:C06S91. doi:10.1029/2006JC004067

Yuan X, Martinson D (2001) The Antarctic dipole and its predictability. Geophys Res Lett 28:3609–3612

Zwally HJ, Comiso JC, Parkinson CL, Cavalieri DJ, Gloersen P (2002) Variability of Antarctic sea ice 1979–1998. J Geophys Res 107:3041. doi:10.1029/2000JC000733